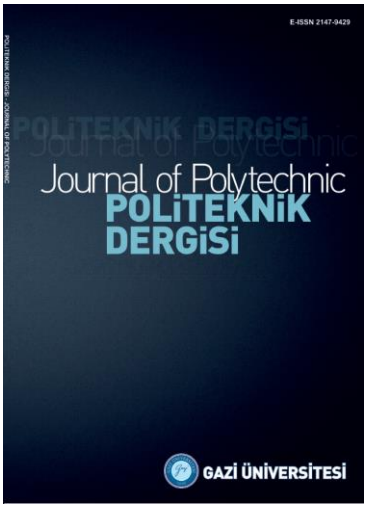


**POLİTEKNİK DERGİSİ**

***JOURNAL of POLYTECHNIC***

ISSN: 1302-0900 (PRINT), ISSN: 2147-9429 (ONLINE)
URL: http://dergipark.gov.tr/politeknik

# The physical properties of aluminium-7xxx series alloys produced by powder metallurgy method

# *Toz metalurjisi yöntemiyle üretilen aluminyum-7xxx serisi alaşımlarının fiziksel özellikleri*

***Yazar(lar) (Author(s))**: Ayşe Nur ACAR[1], Abdul Kadir EKŞİ[2], Ahmet EKİCİBİL[3]*

*ORCID[1]: 0000-0001-7208-1530*

*ORCID[2]: 0000-0003-2227-8006*

*ORCID[3]: 0000-0003-3071-0444*

**Bu makaleye şu şekilde atıfta bulunabilirsiniz(To cite to this article)**: Acar A.N., Ekşi A. K. ve Ekicibil A., "The physical properties of aluminium-7xxx series alloys produced by powder metallurgy method", ***Politeknik Dergisi***, 21(2): 341-350, (2018).

**Erişim linki (To link to this article):** http://dergipark.gov.tr/politeknik/archive

**DOI:** **10.2339/politeknik.389588**

# The Physical Properties Of Aluminium-7xxx Series Alloys Produced By Powder Metallurgy Method

*Araştırma Makalesi / Research Article*

**Ayşe Nur ACAR[1*], Abdul Kadir EKŞİ[2], Ahmet EKİCİBİL[3]**

[1] The Faculty of Ceyhan Engineering, Department of Mechanical Engineering, University of Çukurova, 01950Adana, TURKEY
[2] TheFaculty of Engineering, Department of Mechanical Engineering, University of Çukurova, 01330 Adana, TURKEY
[3] The Faculty of Arts and Sciences, Departmet of Physics, University of Çukurova, 01330 Adana, TURKEY

(Geliş/Received : 17.02.2017 ; Kabul/Accepted : 15.03.2017)

**ABSTRACT**

Alumix-431 materials were prepared by cold and warm compaction method applying 350-400 MPa pressures at RT (room temperature) 50 and 80°C temperatures. The density measurements of materials were performed; the thermoelectric properties of materials were investigated at 5-300K under the He atmosphere, and the relationship between the measurements and sample properties was examined. The measurements of thermoelectric properties showed that maximum resistivity [Alumix -431-1] and thermal conductivity [Alumix -431-6] values were obtained 0.161Ωm and 24.31W/Km, respectively at 285-295K temperature ranges and minimum electrical resistivity and thermal conductivity values were obtained on Alumix-431-6 and Alumix-431-1 samples, respectively. It was observed that Seebeck coefficient values varied mostly from negative sign to positive sign indicated dominate from carriers. The maximum Figure of merit value was determined as $18.71\times10^{-2}$; on the Alumix-431-5 alloy at 96.904K

**Keywords: Cold and warm compaction, powder metallurgy thermoelectric properties, Al-7xxx alloys.**

# Toz Metalurjisi Yöntemiyle Üretilen Aluminyum-7xxx Serisi Alaşımlarının Fiziksel Özellikleri

**ÖZ**

Alumix-431 malzemeleri; oda sıcaklığında (RT) ve 50,80°C sıcaklıklarında 350-400MPa basınç uygulayarak soğuk ve sıcak presleme yöntemiyle hazırlanmıştır. Malzemelerin yoğunluk ölçümleri yapılmıştır ve termoelektrik ölçümleri He atmosferi altında 5-300K sıcalık aralığında gerçekleştirilmiştir. Termoelektrik ölçümlerinde sonuçlar maksimum elektriksel öz direnç ve maksimum termal öz iletkenlik sırasıyla 285-295K sıcaklık aralığında Alumix-431-1 malzemesinde 0.161Ωm ve Alumix-431-6 malzemesinde 24.31W/Km olarak kaydedilmiştir. Minimum elektriksel öz direnç ve termal öz iletkenlik sırasıyla Alumix-431-6 ve Alumix-431-1 malzemelerinde elde edilmiştir. Seebeck katsayısı taşıyıcıların yoğunluğuna bağlı olarak pozitif değerden negative değere değişim göstermiştir. Maksimum performans katsayısı Alumix-431-1 alaşımında 96.904K sıcaklığında $1.871\times10^{-2}$ olarak saptanmıştır.

**Anahtar Kelimeler: Soğuk ve sıcak presleme, toz metalurjisi, termoelektrik özellikler, Al-7xxx alaşımlar.**

## 1. INTRODUCTION

Powder compaction is an attractive forming process, because it presents an approach to net-shape and near net-shape manufacturing [1]. On the many powder compaction methods; for obtaining high density mass, providing the required shape and dimensional control the plastically deformed metal powders are pressed. There are two main powder compaction methods whether applied pressure or not; *i)* pressure applying compaction methods such as cold and warm compaction, double pressing-sintering,isostatic pressing and powder forging, *ii)*pressureless compaction methods such as slip casting and tape casting [2]. In this study; on the preparing of materials, cold and warm compaction methods, as powder compaction methods, were applied and compared the mechanical and physical properties of cold and warm compacted alloys. As known; cold compaction method is applied owing to the directly affect to other processes such as the product density, allow adsorption, diffusion of liquids such as oil and in addition to lead to carrier mobility and warm compaction method is also used due to provide good properties such as higher strength and fatigue strength, tolerances to dimensional variances, grain refinement and increasing Figure of merit (ZT) related to the lattice thermal conductivity [3-6].

The thermoelectrical efficiency of material is evaluated in terms of thermoelectrical Figure of merit (ZT). Effective Figure of merit is provided the high electromotive power Seebeck coefficient (α) ($\alpha=\Delta V/\Delta T$) needed high voltage; high electrical conductivity (σ) and low electrical resistivity (ρ) [$\rho = 1/\sigma$] required to reduce the internal resistance of material; low thermal conductivity [κ] necessitated the large temperature range between two ends of materials [7,8]. ZT is given as follow:

*Sorumlu Yazar (Corresponding Author)
e-posta : anacar@cu.edu.tr

$$ZT = \frac{\alpha^2 T}{\rho\kappa} \quad (1)$$

All properties such as Seebeck coefficient, electrical resistivity, and thermal conductivity are determined by electronic structure and scattering of charge carriers (electrons and holes) and therefore this properties are independently not controlled [9].

In this study; Alumix-431 alloy used is an Al-7xxx series alloy and applied commonly on the air and automotive industry owing to the low density, high strength and hardness and also excellent workability capability [10-12]. The structure of Alumix-431 alloy is included of zinc, copper and magnesium besides of aluminium. For Alumix-431 alloy, zinc is significant alloying addition and, is supporting material for precipitation hardening. Also zinc is dissoluble in aluminum [13]. Because of intrinsic foundry problems such as macrosegregation and cracking, an applied practical limit is about 8wt%, for conventional cast materials [14]. Such as zinc element, copper plays also role as supporting material to precipitation hardening and in order to provide the wetting behavior of the liquid phase of aluminium [13]. Both copper and zinc containing Al alloys have been commonly applied in aerospace, automotive, textile engineering *etc.* and have a high strength/weight ratio [15]. The Al-7xxx alloys are susceptible to localize corrosion because, there are the strengthening phases such as $MgZn_2$, $AlMg_3Zn_2$, $Al_3CuZn$ [15]. Magnesium element is the lightest material and shows superior features such as high dimensional stability and thermal conductivity, good formability and recyclability, inadequate corrosion resistance due to high reactivity. Magnesium and its alloys are characterized by way of low hardness and wear resistance, therefore, their useful areas are limited to mechanical parts worked under static conditions such as casing, housing [16]. Even at 0.5% magnesium element level possesses positive effect on shrinkage by way of decreasing the oxide, enabling diffusion and metal/metal contact at particle interfaces [13].

On Al-7xxx alloys; the electrical resistivity behaviour has inclusively been studied during the pre-precipitation stage. Ferragut et al. examined the early stages of pre-aging in an Al-Zn-Mg-Cu alloy with electrical resistivity at near room temperature. In the early stages of pre-aging, it was determined, the increasing of electrical resistivity. There is susceptible of electrical resistivity to the microstructural factors consisting of vacancy concentration, solute concentration in the matrix, precipitate (or cluster) size and precipitate volume fraction. Resistivity varies to the increase of the electron scattering resulting from a non-random distribution of the formed pre-precipitates. Authors determined the enoughly changing of the resistivity in the sense of a JMA(Johnson-Mehl-Avrami) type for volume fraction growth of the Guinier-Preston zones or pre-precipitate solute cluster formed [17].Guyot and Gotignies investigated precipitation kinetics and features size and volume fraction, mechanical strength and electrical conductivity of AlZnMgCu alloys by in-situ SAXS experiments [18]. Salazar-Guapuriche et al. studied the mechanical properties such as tensile strength, proof strength hardness and the transport properties such as electrical conductivity of Al alloy 7010 under various temper and ageing conditions so as to associate strength with hardness and electrical conductivity [19]. Massadier et al., measured the TEP value of a 6061-Al alloy during isothermal ageing performed between 200 and 500°C. They expressed permitting the TEP kinetics an evaluation of the residual concentration of solute in the final equilibrium state and stated the reflecting of variations of TEP the microstructural transformations occurring in the alloy [20]. Sun et al. investigated the solution treatment and aging of a 2024 Al alloy using TEP technique and compared to obtained results by microhardness and optical microscopy. They stated the varying of the TEP value with solution treatment temperature and duration during solution treatment and variations in the solubility of the alloying elements in the α-Al [21]. The purpose of this study is to investigate the mechanical and physical properties of Alumix-431 (Al-5.5Zn-2.5Mg-1.5Cu) material which is the Al-7xxx series alloy and prepared utilizing the traditional press and sintering process in various pressure and temperatures.

## 2. EXPERIMENTAL PROCEDURE

In this study, the compacted Alumix-431 material obtained from the powder which is the alloy of Al-7xxx series alloy and acquired from Ecka Granules in Germany was utilized. In the below Table 1 the chemical composition of Alumix 431 powder is given.

**Table 1.** The Percentage of the Chemical Composition of Alumix-431.

| ***Chemical Composition,% (density 2.786 g/cm$^3$)*** | |
|---|---|
| Al | 89.0 |
| Cu | 1.5 |
| Mg | 2.5 |
| Zn | 5.5 |
| Lubricant | 1.5 |

Previously, the components of powder in Table 1 chemical composition (Al-5.5Zn-2.5Mg-1.5Cu) which are roughly weight of 15 g are blended to place the blanks, until a homogeneous mix by the lubricants. Obtained a homogeneous mixture placed into prismatic die (10×10×55) mm$^3$ which has approximately a weight of 3.5 g with an accuracy of 0.001 g for static properties. Alumix-431 alloys were pressed up 350 and 400 MPa pressures at various temperatures; room temperature (RT), 50° C and 80° C. In order to observe mechanical properties; the density measurements of green Al alloys was assessed. Densities of green parts pressed were measured by Classical Method and the Archimedes Principle which is water displacement technique, using

Precisa 320XT series for analytical and precision balances which has 1/10.000 precision of scale.

In order to measure the physical properties such as thermal conductivity, Seebeck coefficient, electrical resistivity, in the literature; there are the measurement methods (22-24). In this study, the physical properties were performed on the PPMS-QD (Physical Properties Measurement –Quantum Design). In PPMS; thermal conductivity is measured by monitoring the decrease of temperature because of heat passing through the sample; in order words by direct transient method where the variations (increase and decrease) in temperature between two thermometers (25,26). Seebeck coefficient measurement is performed from attaching four ends to the sample by conducting silver epoxy. Whereas one end at a constant temperature by continuing good the conductivity with a low temperature reservoir is holded; at the other end of the specimen applying of heat is occurred a temperature gradient (27). For measuring of electrical resistivity; there are several options in PPMS. The measurement of electrical resistivity is made by adding a configurable resistance bridge board, called the user bridge board to PPMS. To specific system, none of the four channels on the user bridge board is allocated; therefore, all four channels exist in order to make four-end resistance measurements on the PPMS (28). The cold and warm compacted specimens (10×55×10) mm cut to take place PPMS machine.

The obtained materials were enumerated to increasing pressures and temperatures. In following chart; designated materials were given;

**Table 2.** The preparation conditions of Alumix-431.

| ***Sample Names*** | ***Preparation conditions*** |
|---|---|
| Alumix-431-1 | 350MPa, RT |
| Alumix-431-2 | 350 MPa, 50°C |
| Alumix-431-3 | 350 MPa, 80°C |
| Alumix-431-4 | 400MPa, RT |
| Alumix-431-5 | 400MPa, 50°C |
| Alumix-431-6 | 400MPa, 80°C |

## 3.RESULTS AND DISCUSSION

### 3.1. Powder Morphology and Characterization

#### 3.1.1. Particle Size Distribution of Alumix-431 Alloy Powder

In Figure 1, the SEM image and the cumulative particle size distribution of Alumix-431 alloy powder are presented. The SEM image of Alumix-431 alloy powder obtained by Nova NanoSEM 650 machine and the cumulative particle size distribution of this powder was determined using BT-9300HT Laser Particle Size Analyzer with water medium and Mie scattering. As observed in SEM image; particles of Alumix-431 powder have irregular shape. The irregular shape of Alumix-431 particles is provided more compactibility on compressing of alloys compared to the circular shape [29]. The particle size distribution is important for packing and sinterability [30,31]. Because of consisting of a variety of particle size of ranges, the distribution of Alumix-431 alloy is observed the multimodal distribution [31]. In this study, the mean particle size of Alumix-431 is obtained of 67.458 μm.

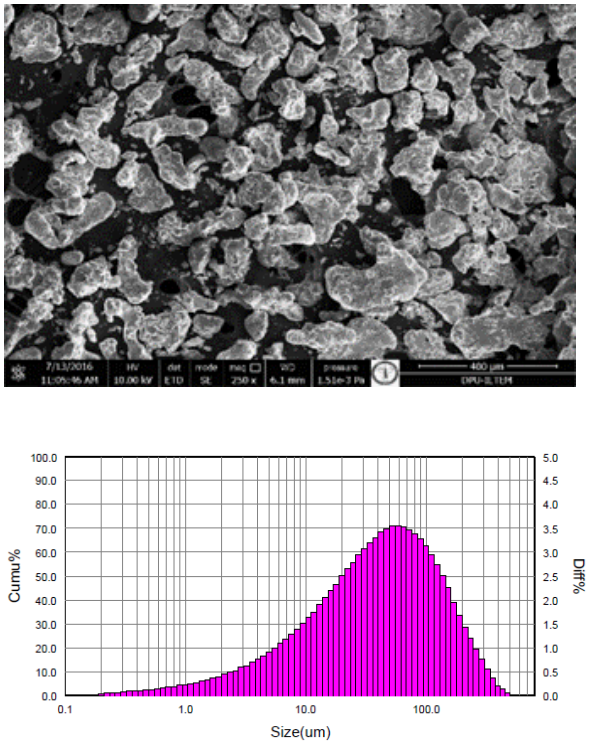


**Figure 1.** The SEM image and cumulative particle size distribution of Alumix-431 alloy powder

#### 3.1.2. The XRD pattern of Alumix-431 alloy powder

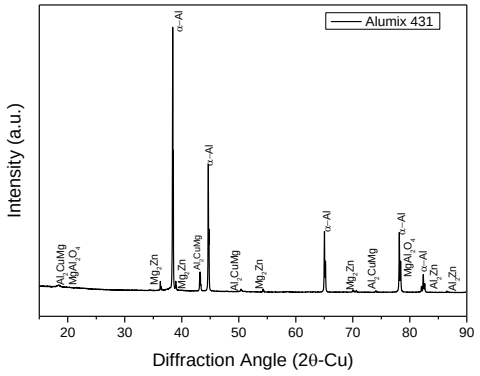


**Figure 2.** The XRD pattern of Alumix-431 alloy Powder

In Figure 2, there is an apparent of the phase analysis of Alumix-431 powder obtained XRD (X-Ray Diffraction) using PANalytical EMPYREAN model XRD Device

with [CuKα] radiation (λ=1.54Å),tube voltage of 40 kV, tube current of 35mA and scanning rate of 0.02°/min. The Figure 2 was showed the strong peaks of main peak of Al and the weak peaks of other elements of Mg,Zn,Cu. Sometimes, on strong peaks, the other elements were locally available with aluminum. In Figure 2, α-Al as the main phase, η ($MgZn_2$) phase as the second main phase and having hexagonal closed packed (HCP) eutectic structure, S($Al_2CuMg$) phase having the orthorombic eutectic structure, $Al_2Zn$ phase on final peaks and also locally placed spinel phases on peaks are observed [32-33]. The dissolving of $Al_2CuMg$ is diffuculty than $MgZn_2$ phase. The $MgZn_2$ phase is important due to the obstacle dislocation movement; for this reason it will be increased mechanical features [34,35]. On the spinel phase, it was thought out the Mg element will be dissolved in to grain boundary because of the reaction of Mg and oxide layer on aluminum particle. On the final peaks, the observation of $Al_2Zn$ alloys is considered due to contain Zn embedded in aluminium.

#### 3.1.3.Optic Microscope (OM) Images of Alumix-431 Alloy

The optical microscope images of Alumix-431-1 material are shown in Figure 3, it was showed the grain and grain boundaries of Cu, Mg, Zn, Al elements prominently. It was appeared that an equixed grains and two types with apparent origins, the first generated at the grain boundaries during the solidification process caused to segregation of the alloying elements when the second phase is widely formed near the grain boundaries. Many coarse precipitates are distinct within the constituted grains [36].

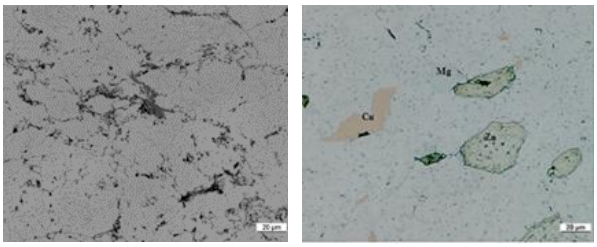


**Figure 3.** Optical microscope images of Alumix-431-1 sample with materials [20µm] [350MPa/ RT].

### 3.2. Mechanical Properties of Alumix-431 Alloys

#### 3.2.1. The Green Density of Alumix-431 Alloys

For materials produced from powder metallurgy (PM) methods, the density measurements are crucial because of influencing the mechanical and physical properties of the materials. As known; to increase the performance of PM part, the best way is the rising of the density [15]. The rising density is caused to propose the various treatments; *i)* for high and uniform densities and decreasing of residual stresses and providing magnetic properties; warm compaction (W/C) method has been utilized. *ii)* As known, in the W/C method, material powder is preheated and compacted in a heated material. *iii)* to fabricate both cost-effective and highly dense sintered products, W/C process has been developed [37]. The results of the density measurements of Alumix-431 samples showed that the density of the samples increase with increasing compacting pressure. To move rearrangement and deform of powder particles, the rising of the compacting pressure is beneficial. Increasing of density is also closely associated with the state of lubricant based on the temperature [38]. It was presented the increasing of density with increasing pressures and in Figure 4, it was observed that the density of alloys was firstly increased and then decreased with the increasing of temperature on both pressures. With the rising temperature, porosity is decreased because of reducing of volume of compacted parts and gaining particles and non-varied weight (see in Figure 4). These conditions increase the density of samples [39]. The decreasing of density is recommended the increasing of resistance to density with reducing of porosity [40]. The highest density value of samples was indicated at compacted specimens on the 400MPa/50°C (Alumix-431-5) conditions.

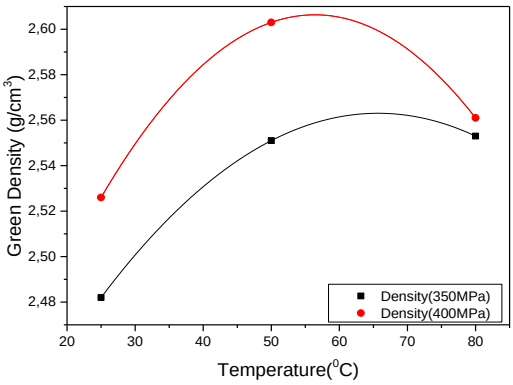


**Figure 4.** Green Density related to the Temperature of the Alumix-431 samples.

### 3.3. The Physical Properties of Alumix-431 Alloys

In this study, the physical properties of Alumix-431 alloys are performed on the PPMS-Quantum Design (Physical Property Measurement System) at 5-300K temperature under He atmosphere. The physical properties obtained from PPMS for Alumix-431 alloys were electrical resistivity, thermal conductivity and Seebeck coefficient. Figure of merit was calculated from acquired properties according to the Wiedemann-Franz Law, as known.

#### 3.3.1. The Electrical Resistivity and Thermal Conductivity of Alumix-431 alloys

As known, electrical resistivity (ρ) is resistance to flow of electric current and electrical resistivity property is based on the material type and temperature. Materials having low electrical resistivity permit the movements of electrical current. Metals have low electrical resistivity and generally give $10^{-7}$(Ωm) electrical resistivity values whereas insulators have $10^{10}$-$10^{20}$ (Ωm) electrical resistivity values, namely presents high electrical resistivity property. Semiconductivity materials also

posses averaged resistivity and have range of $10^{-4}$-$10^{6}$ (Ωm) electrical resistivity values [41].

In this study; on electrical resistivity-Temperature graphs, it was observed the electricity resistivity values of Alumix-431 samples compacted on 350MPa pressure at RT,50,80°C temperatures were higher than the ones of compacted Alumix-431 samples on 400MPa at the same temperatures (see Figs. 5-6). Maximum and minimum electrical resistivity values are obtained on Alumix 431-1 and 5; 6 samples at 5-300K temperature, respectively.

In Alumix-431-1 material, the valleys are prominently appeared according to the other Alumix-431 materials in range from 250 to 200 K temperatures ($1.48\times10^{-2}$ Ωm at 205.05K and $1.392\times10^{-2}$ Ωm at 218. 593 K) and observed in roughly constant. It was considered to such a tendency is attributed to a falling offset of $E_F$ (Fermi Energy) from the valley of the pseudo-gap because of motion of $E_F$ to the location with larger density of states (DOS) causing to the reducing in the electrical resistivity magnitude and also considered [36,37] in Figure 5. Maximum electrical resistivity is obtained in value of $16.1\text{x}10^{-2}$Ω.m at about 299K for Alumix-431-1 specimen. As shown in Figure 5 superconductivity property of materials was considered. In Alumix-431-1, the sharp decreasing was exhibited at about 250K. It was thought on similar behaviour to superconductivity property of materials or structural transition via TEP. Both the constitution and resolution of η'phase and the constitution of η phase a strongly effect on the electrical resistivity. This effect is more than inclined via the development of GP zones [38]. On Alumix-431-2 sample, it was observed the linear increase as temperature rose. Alumix -431-3 samples showed a similar behavior to superconductivity property and same property on the Alumix-431-1 sample. After 225K, the reason for the GP zone generation may be less in concentration of defects (38). Maximum electrical resistivity obtained on the Alumix-431-1 sample(0.161Ωm at 300K).

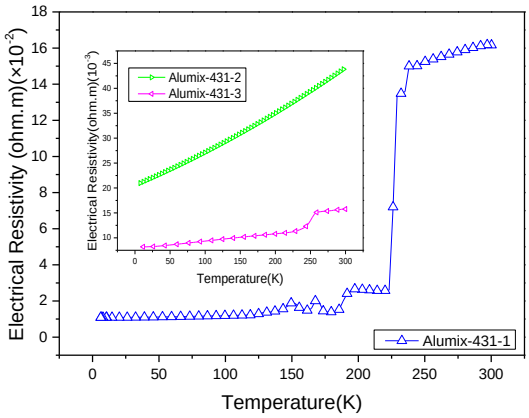


**Figure 5.** The Electrical Resistivity versus Temperature curve of Alumix-431-1, 2 and 3.

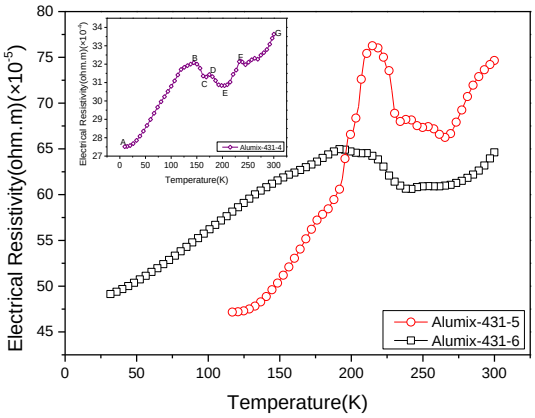


**Figure 6.** The Electrical Resistivity versus Temperature curve of Alumix-431-4, 5and 6.

On Alumix-431-4-5-6 samples, it was observed the phase transition regions in Figure 6. Apparently the phase transition regions was realized on the Alumix-431-4 sample and characterized; AB- metallic transition because of the scattering of electrons from isotropic centers, BC-DE- semiinsulating transition the constitution of electron hole drop or quantum well, CD-EF- semimetallic transition anisotropic scattering of electrons from gap or cracked sites, FG- hybrid transition because of both the metalloid diffusion and semimetallic diffusion [45] (see in Figure 6). On Alumix-431-6 sample, it was appeared the variation of BC and CD phase transition regions decreases as temperature rises. The increase in resistivity for Alumix-431-5 system (at temperature range 5-300K) is explained lowers the resistivity of from $6.624\times10^{-4}$ Ωm at 251.88K, $6.807\times10^{-4}$ Ωm at 207.24K and $4.717\times10^{-4}$ Ωm at 12.88K, and produces a metallic conductors shown in Figure 6. In Alumix-431-6 specimen, the decrease in resistivity is also observed in $6.457\times10^{-4}$ Ωm at 203.16K, $6.0657\times10^{-4}$ Ωm at 240.068K and $6.0807\times10^{-4}$ Ωm at 140.60 K. These observings show that within these temperature ranges, there is a composition attribute that obtained semiconducting features while metallic behavior is sighted on both sides of these ranges (Figures 6) [46]. In Figures 6, it was observed the increasing of the resistivity due to the increasing of the lattice distortions, causing to the carrier concentration and decreasing of mobility [47,48].Minimum electrical resistivity obtained on the Alumix-431-6 sample( 49.145 Ωm at 31.68K) and then , on the Alumix-431-5 sample( 47.174 Ωm at 116.86K).

A high quality thermoelectric material must be necessitated both a low electrical resistivity and a high thermopower and a low thermal conductivity. According to the Wiedemann-Franz law, total thermal conductivity is expressed by the transporting heat of carriers (holes and electrons) ($\kappa_e$) and the phonons travelled via the lattice ($\kappa_{ph}$) [49].

$$\kappa_{total}=\kappa_e+\kappa_{ph} \quad (2)$$

High thermal conductivity worsens the overall the thermoelectric performance. To provide thermoelectric performance of alloys, the thermal conductivity is decreased [50].

On all Alumix-431 samples, it was observed the increasing of thermal conductivity as rising of pressure and temperature and the thermal conductivity of compacted alloys on 350MPa were higher than the ones of compacted alloys on 400MPa. Increasing of thermal conductivity is occurred from rapidly both decreasing of electrical resistivity and strong increasing of the electronic thermal conductivity component ($\kappa_e$).

As generally examining Figs. 7 and 8; the low thermal conductivity was obtained on the Alumix-431-1 alloy compacted on the low pressure and temperature and it was recommended that low thermal conductivity was meant the having a higher content of solute elements in the α-Al matrix (0.260W/Km at 6.19 K). It was also observed the low thermal conductivity on Alumix-431-1 samples according to other alloys considering dominating via grain boundary and impurity scattering and considered the low thermal conductivity due to the occurring of heat transfer, embedded alloying elements the movements of free electrons that are primary source in order to transport heat in metals and decreasing free path [50,51]. The decreasing thermal conductivity is caused to the decreasing of the electronic thermal conductivity according to Wiedemann-Franz Law (see Fig 7). Maximum thermal conductivity was acquired in value of 24.31 W/Km at 297.065 K for Alumix 431-6 specimen. High thermal conductivity is led to low porosity position and large grain size because of decreasing grain boundary and spreading of phonons[52]. On Alumix -431 -6 sample, it also appeared having high density property after that one of compacted Alumix-431-5 sample on 400MPa/50°C. With increasing temperature, at Alumix-431-6 sample the thermal conductivity increased linearly and did not show any peak based on the microstructural change and, due to the rapidly decreasing of solid solubility of Cu atoms in the α-Al matrix, this case was occurred to increasing of thermal conductivity [53].

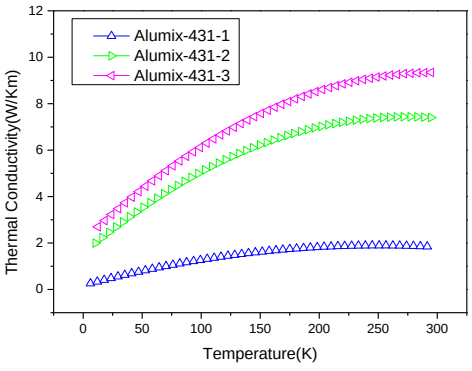


**Figure 7.** The Thermal Conductivity versus Temperature curve of Alumix-431-1, 2 and 3.

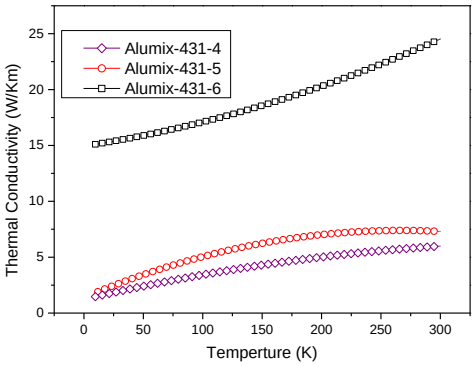


**Figure 8.** The Thermal Conductivity versus Temperature curve of Alumix-431-4, 5and 6.

### 3.3.2. The Seebeck Coefficient of Alumix-431 alloy

The Seebeck coefficient value is significant physical feature because of enhancing the potential performance of thermoelectric materials and quite sensitive to electronic structure [50]. In transport property, a change is showed as the sign and the magnitude of S(T) change rapidly demonstrating charge carriers varied from n-type to p-type [54].At a temperature (T) the Seebeck coefficient is important value for electronic structure is expressed by Mott's formula;

$$S(T) = T\left(\frac{\partial ln\sigma(E)}{\partial E}\right)_{E_T=E_F} \quad (3)$$

σ(E) is expressed the electrical conductivity-reciprocal of electrical resistivity-as a function of function energy. According to the formula; Seebeck coefficient is suitable to the incline of DOS at the Fermi level and is generated via both electrons and holes [54]. The negative effect of Seebeck coefficient is occurred by the increasing of the electrons whereas the positive effect of Seebeck coefficient is acquired the increasing the carriers. Increasing of Seebeck coefficient is also recommended with inducing to the lower carrier concentration and decreasing of mobility on the same as electrical resistivity increasing values [48].

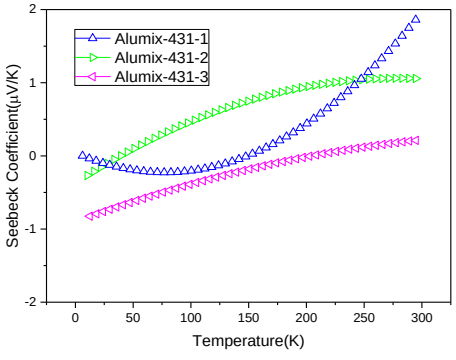


**Figure 9.** The Seebeck Coefficient versus Temperature curve of Alumix-431-1, 2 and 3

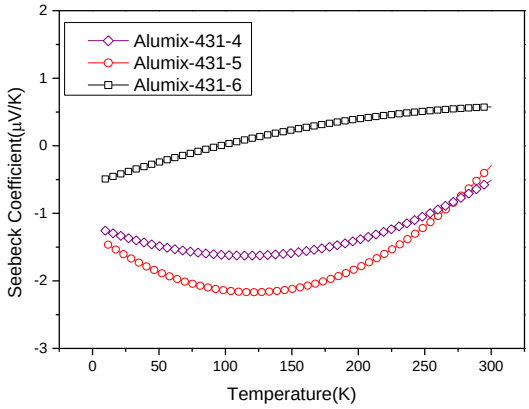


**Figure 10.** The Seebeck Coefficient versus Temperature curve of Alumix-431-4, 5 and 6

In Figures 9 and 10; it was observed ; on compacted Alumix-431 alloys on 350MPa, the Seebeck Coefficient values of Alumix-431-2 and 3 samples were continuously increased and on other compacted alloys on 400MPa, the value of only Alumix-431-6 was increased and also appeared the one of other sample firstly decreased and then increased. Alumix-431-2, 3, 6 samples showed the positive Seebeck coefficient occurred from holes stemmed from a powerful energy based on the hole mobility and caused to the positive TEP at higher temperatures. Reasons of increasing of conductivity (see Figures 7 and 8) and decreasing of Seebeck coefficient (see Figures. 9-10) are the formation of defects when applied sintering in reduced atmosphere and variation of carrier concentration on Alumix-431-1, 4, 5 samples [50].

For Alumix-431-1, 2, 3 and 6 samples, Seebeck coefficient values are neutralized at 59.49K, 32.59K, 198.67K and 164, 23K where neutralize of the Seebeck coefficient values respectively (see Figures 9 and 10). In Fig.9, the high Seebeck Coefficient was acquired on the Alumix-431-1 sample and the Seebeck Coefficient value firstly decreased due to the mostly electron concentration and then increased due to the carrier concentrations. The Seebeck coefficient value of this alloy was changed from n-type to p-type. At final temperature, the alloy was showed on the p-type mostly carrier concentration and gave the value 1.8663 μV/K at 294.90K. On the same time, high Seebeck coefficient is also corresponded to high porosity specimen and grain size because of the rising spreading carriers by the impurities and flaws that increased impurities and flaws caused to reducing the grain boundaries [52]. It was observed on Alumix -431-1 sample having the low density (2.482g/cm$^3$) according to the other samples. In Figure 10, Alumix-431-5 had high Seebeck coefficient, presented n-type because of the mostly electron concentration and also gave 2.165μV/K at 121.49K.

### 3.3.3. The Figure of Merit of Alumix-431 alloys

The dimensionless thermoelectric figure of merit (ZT) summed up the thermoelectric properties is important factor in selecting material for TEP (thermoelectric power) generation and coolant [46]. As above expressed by formula; the Figure of merit (ZT) is calculated from electrical resistivity, Seebeck coefficient and thermal conductivity. The high ZT value is provided by low electrical resistivity and thermal conductivity and high Seebeck coefficient values.

On Figure 11; it was observed that the value of Alumix-431-1 sample was firstly decreased and then increased to final temperature and on the Alumix-431-3; the value changed reverse of the value of Alumix-431-3 sample. Also on the Alumix-431-2 sample, it was appeared increasing of the Figure of merit change. Minimum Figure of Merit was obtained on the Alumix-431 -3 sample due to low Seebeck Coefficient and high thermal conductivity (0.0055 $\times 10^{-3}$; 179.63K).On the other Figure 12; the Figure of merit values of Alumix-431-4 and -5 samples were firstly increased and then decreased. As is seen Figure 12; the maximum Figure of merit was obtained on Alumix-431-5 sample due to the low electrical resistivity and thermal conductivity and high negative Seebeck coefficient values according to the other all Alumix-431 samples ($1.871\times10^{-2}$; 96.904K). Also, on the Alumix-431-6 sample; Figure of merit of alloy was not showed continuously whether increasing or not the decreasing even though locally fluctuates and also given low values due to high thermal conductivity and low Seebeck Coefficient values even though minimum electrical resistivity.

On the all Alumix-431 samples; it was also observed the valleys due to the phase transition phase transition variation from η phase to η' phase [55].

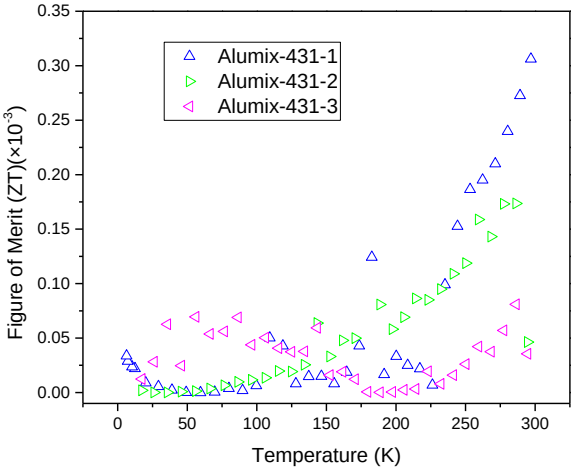


**Figure 11.** The Figure of Merit versus Temperature curve of Alumix-431-1, 2 and 3

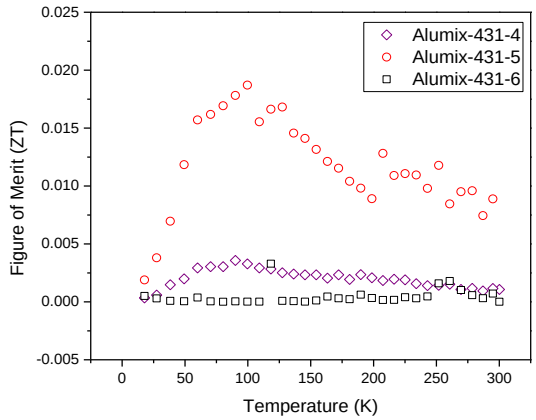


**Figure 12.** The Figure of Merit versus Temperature curve of Alumix-431-4, 5 and 6

## 4. CONCLUSIONS

The Alumix-431 materials prepared by cold and warm compaction method by applying to 350-400 MPa pressures at RT, 50, 80°C temperatures were investigated with regard to the density and thermoelectrical properties at 5-300K temperatures. It were attained following principal results;

**1.** The particle size characterization presents the irregular shape of particle size, multimodal distribution and mean particle size of 67.458µm

**2.** The high green density value were acquired at the compacted specimens on the 400MPa/50°C condition (Alumix-431-5).

**3.** The obtained physical experimental results show that at temperature range of 5-300 K under He atmosphere;

**a.** The maximum electrical resistivity and thermal conductivity were acquired 0.161Ωm [Alumix-431-1] and 24.31W/Km, [Alumix-431 -6] respectively and, minimum electrical resistivity and thermal conductivity values obtained on Alumix -431- 6, and 1 alloys, respectively.

**b.** The Seebeck Coefficient values changed mostly negative sign to positive sign due to dominate from carriers on Alumix-431 alloys compacted on 350MPa, at RT, 50 and 80°C temperatures, while the other Alumix-431 samples compacted on 400 MPa at same temperatures, except for Alumix-431-6 sample, showed giving the negative Seebeck Coefficient values. It was also observed the Alumix-431-6 samples compacted on high pressure and temperature, having the positive Seebeck Coefficient values.

**c.** Maximum Figure of Merit was obtained on the Alumix-431-5 sample ($1.871\times10^{-2}$;96.904K);minimum Figure of Merit also was acquired on the Alumix-431-3 sample ($0.0055\times10^{-3}$; 179.63K).

## ACKNOWLEDGEMENTS

This work is supported by the Research Fund of Çukurova University, Adana, Turkey, under grant contract no. ÖYP-2090.

## REFERENCES

**[1]** Rahman M.M., Nor S.S.M. and Rahman H.Y., Technical Report, ‘’Investigation on the effect of lubrication and forming parameters to the green compact generated from iron powder through warm forming route‘’, ***Materials and Design,*** 32: 447-452,(2011)

**[2]** Melúch L., ‘’Warm compaction of aluminum alloy alumix 123‘’, ***Thesis of Doctoral of Philosophy***, University of Birmingham, page 237,(2009)

**[3]** Jafar-Salehi E., Ghasempoor A. and Eslamian M.,‘’Experimental study and predictive modelling of cold compaction green density in powder metallurgy of stainless steel components‘’, ***Powder Metallurgy***, 56: 3, 208-215,(2013)

**[4]** Cao G., Zhang Q. and Brinker C.J., ‘’Annual review of nano research ’’ Volume 3, ***World Scientific Publishing***, Singapore, page 568, (2010)

**[5]** Rahman M.M., Ariffin A.K., Nor S.S.M. and Rahman H.Y.,‘’Powder material parameters establishment through warm forming route‘’, ***Materials and Design*** 32: 264-271, (2011)

**[6]** Bhuiyan M.H., Kim T.-S. Koo J.M. and Hong S.-J., ‘’Microstructural behavior of the heat treated n-type 95% $Bi_2Te_3$–5% $Bi_2Se_3$ gas atomized thermoelectric powders‘’, ***Journal of Alloys and Compounds*** 509: 1722–1728,(2011)

**[7]** Zevalkink A., Toberer E. S., Zeier W. G., Flage-Larsen E. and Snyder G.J.,‘’$Ca_3AlSb_3$: An inexpensive, non-toxic thermoelectric material for waste heat recovery‘’, ***Energy Environ.Sci.***, 4: 510-518, (2011)

**[8]** Ohta H., Sugiura K. and Koumoto K., ‘’Recent Progress in Oxide Thermoelectric Materials: p-Type $Ca_3Co_4O_9$ and n-Type $SrTiO_3$–‘’***Inorg. Chem.***,47, 8429–8436, (2008)

**[9]** Snyder G.-J. and Toberer E.S., ‘’Complex thermoelectric materials‘’, ***Nature Materials,*** vol.7.: 105-114,(2008)

**[10]** Fang S.F., Wang M.P. and Song M.,‘’An approach for the aging process optimization of Al–Zn–Mg–Cu series alloys‘’. ***Materials and Design***, vol. 30:2460-246, (2009)

**[11]** Jia Y., Cao F., Ning Z., Guo S., Ma P. and Sun J., ‘’Influence of second phases on mechanical properties of spray deposited Al–Zn–Mg–Cu alloy‘’. ***Materials and Design***, vol. 40: 536-540, (2012)

**[12]** Liu Y., Jiang D., Li B., Yang W. and Hu J., ‘’Effect of cooling aging on microstructure and mechanical properties of an Al–Zn–Mg–Cu alloy‘’, ***Materials and Design***, vol. 57: 79-86, (2014)

**[13]** Ekşi A.,Veltl G., Petzoldt F., Lipp K. and Sonsino C.M., ‘’ Tensile and fatigue properties of cold and warm compacted alumix 431 alloy‘’, ***Powder Metallurgy***, 200A, vol 47, no.1: 60-64, (2004)

**[14]** Feng W., Baiqing X., Yongan Z., Hongwei L., and Xiaoqing H. ‘’ Microstructural development of spray deposited Al-Zn-Mg-Cu alloy during subsequent porosity‘’, ***Journal of Alloys and Compounds***,477: 616-621, (2009)

**[15]** Xue W., Wang–Tian H., and Lai Y., ‘’Corrosion behaviour and galvanic studies of microscopic oxidation films on Al-Zn-Mg-Cu alloy‘’, ***Surface ad Coatings Technology*** 201: 8695-8701, (2007)

**[16]** Mola R., ''Fabrication and microstructural characterization of Al/Zn enriched layers on pure magnesium'', ***Material Characterization***,78: 121-128, (2013)

**[17]** Ferragut R.,Somoza A. and Torriani I., ''Pre-precipitation study in the 7012 Al-Zn-Mg-Cu Alloy by electrical resistivity'', ***Material Science and Engineering***, A334:1-5, (2002)

**[18]** Guyot P. and Gottigines L., ''Precipitation kinetics, mechanical strength and electrical conductivity of AlZnMgCu alloys'', ***Acta Mater*** vol.44, no 10: 4161-4167, (1996).

**[19]** Salazar-Guapuriche M.A., Zhao Y.Y., Pitman A., and Greene A.,''Correlation of strength with hardness and electrical conductivity for aluminum alloy 7010'', ***Materials Science Forum***, vols 519-521:853-858, (2006)

**[20]** Massadier V., Epicier T. and Merle P., ''Correlation between the microstructural evolution of a 6061 aluminum alloy and the evolution of its thermoelectric power'', ***Acta Mater.,*** 48,:2911-2924,(2000)

**[21]** Sun D., Sun X.-C. and Northwood D.O., Sokolowski J.-H.,''Thermoelectric power characterization of a 2024 aluminum alloy during solution treatment and aging'', ***Materials Characterization*** 36:83-92, (1996)

**[22]** Ahiska R. and Ahiska K., ''New method for ınvestigation of parameters of real thermoelectric modules'', ***Energy Conversion and Management*** 51:338–345, (2010)

**[23]** Ahiska R. , Ahiska G. and Ahiska K., ''Analysis of a new method for measurement of parameters of real thermoelectric module employed in medical cooler for renal hypothermia'', ***Instrumentation Science and Technology***, 37: 102–123, (2009)

**[24]** Ahiska R., ''New method for ınvestigation of dynamic parameters of thermoelectric modules'', ***Turk J Elec Engin***, Vol.15, No.1,51-65 (2007).

[**25]** Sebek J. and Santava E., ''Influence of the sample mounting on thermal conductance measurements using PPMS TTO option'', ***Journal of Physics: Conference Series***,150:012044,1-4, (2009)

**[26]** Borup K.A., Boor J. de. Wang H., Drymiotis F., Gascoin F., Shi X., Chen L., Fedorov M.I., Müller E., Iversen B.B. and Snyder G.J., ''Measuring thermoelectric transport properties of materials'', ***Energy Environ. Sci***., 8: 423–435, (2015)

**[27]** Hettinger J.D., Lofland S.E., Finkel P.,Meehan T., Palma J., Harrell K.,1 Gupta S., Ganguly A., El-Raghy T. and Barsoum M.W.,''Electrical transport, thermal transport, and elastic properties of $M_2AlC$ (M=Ti, Cr, Nb, and V) '' ***Physical Review B,*** 72:115120, (2005)

**[28]** Physical Property Measurement System Resistivity Option User's Manual, Quantum Design s.48

**[29]** Rudianto H., Joo J.K., Sun Y.S., Jin K.Y. and Diouhy I., ''Mechanical properties of sintered of Al-5.5Zn-2.5Mg-0.5Cu PM Alloy'', ***Materials Science Forum,*** vols 794-796: 501-507,(2014)

**[30]** Liu Z.Y., Sercombe T.B. and Schaffer G.B., ''The effect of particle shape on the sintering of aluminum '', ***Metall. Mater. Trans.*** A38: 1351–1357,(2007)

**[31]** Buranasrisak P. and Narasingha M.P., ''Effects of particle size distribution and Packing characteristics on the preparation of highly-loaded coal-water slurry'', ***International Journal of Chemical Engineering and Applications***, vol. 3, no. 1: 31-35, (2012)

**[32]** Naeem H.T., Mohammad K.S., Ahmad K.R. and Rahmat A.,''Characteristics of Al-Zn-Mg-Cu alloys with nickel additives synthesized via mechanical alloying, cold Compaction and heat treatment'', ***Arap J.Sci. Eng.***, 39: 9039-9048, (2014)

**[33]** LaDelpha A.D.P., Neubing H. and Bishop D.P., ''Metallurgical assessment of an emerging Al-Zn-Mg-Cu P/M alloy'', ***Materials Science and Engineering,*** A 520 :105-113, (2009)

**[34]** Mondal C. and Mukhopadyay A.K., ''On the nature of $T(Al_2Mg_3Zn_3)$ and $S(Al_2CuMg)$phases present in as-cast and annealed 7055 aluminum alloy'', ***Materials Science and Engineering,*** A391:367-376, (2005)

**[35]** Rudianto H., Jang G.J., Yang S.S., Kim, Y.J. and Dlouhy I., ''Evaluation of sintering behavior of premix Al-Zn-Mg-Cu alloy powder'', ***Advances in Materials Science and Engineering***, volume 2015: 987687, 1-8, (2015)

**[36]** Rudianto H., Jang G.J., Yang S.S., Kim Y.J.and Dlouhy I., ''Effect of SiC particles on sinterability of Al-Zn-Mg-Cu P/M alloy'', ***Archives of Metallurgy and Materials,*** volume 60, ıssue 2 :1383-1385,(2015)

**[30]** Mazzer E.M., Alfonso C.R.M., Galano M., Kiminami C.S. and Bolfarini C., ''Microstructure evolution and mechanical properties of Al–Zn–Mg–Cu alloy reprocessed by spray-forming and heat treated at peak aged condition'', ***Journal of Alloys and Compounds,*** 579: 169–173,(2013)

**[37]** Shokrollahi H. and Janghorban K., ''Effect on warm compaction on the magnetic and electrical properties of Fe-based soft magnetic composites'', ***Journal of Magnetism and Magnetic Materials***, 313:182-186, (2007)

**[38]** Feng S.-S., Geng H.-R. and Guo Zh.- Q., ''Effect of lubricants on warm compaction process of Cu-based composite'', ***Composites: Part B,*** 43: 933–939,(2012)

**[39]** İynen, O., ''The influence of sintering and shot peenıng processes on Alumix 431 Powder materials'', ***Master Thesis***, Çukurova University, Institute of Natural and Applied Sciences, (2009)

**[40]** Gökmeşe G. and Bostan B.,''AA 2014 alaşımında presleme ve sinterlemenin gözenek morfolojisi ve mikroyapısal özelliklere etkileri'',***Gazi Üniversitesi Fen Bilimleri Dergisi,Part:C, Tasarım Ve Teknoloji GU J Sci Part:C*** 1[1]:1-8, (2013)

**[41]** Callister, W.D. Jr. and Rethwisch D.G., ''Material science and engineering'', Eight Edition, ***XXVI John Wiley and Sons Asia Pte Ltd.*** USA, page 974, (2011)

**[42]** Aksan M.A.,Güldeste A., Balcı Y. and Yakıncı M.E.,''Degradation of superconducting properties in $MgB_2$ by Cu addition '', ***Solid State Communications,*** 137: 320–325, (2006)

**[43]** Aksan M.A., Altın S., Balcı Y. and Yakıncı M.E., ''Structural characterization and transport properties of the $HT_c$ $Bi_2Sr_2(Ca,Cd)Cu_2O_{8+\delta}$ glass-ceramic rods'', ***Materials Chemistry and Physics*** 106: 428-436, (2007)

**[44]** Smontara A., Smiljanić I., Bilušić A., Jagličić Z., Klanjšek M., Roitsch S., Dolinšek J. and Feuerbacher M., ''Electrical, magnetic, thermal and thermoelectric properties of the "Bergman phase" $Mg_{32}(Al,Zn)_{49}$ complex metallic alloy'', ***Journal of Alloys and Compounds*** 430: 29–38, (2007)

**[45]** Gormani M.A., Raza S.M., Farooqui N., Ashfaq M. and Ahmed M.A., ''On thermally activated electrical resistivity in metallic glasses'', ***Solid State Communkations,*** vol. 95, no. 5: 329-333, (1995)

**[46]** Tani J.-I. and Kido H.,''Thermoelectric properties of Al-doped $Mg_2Si_{1-x}Sn_x[x\leq0.1]$'', ***Journal of Alloys and Compounds,*** 466: 335-340, (2008)

**[47]** Rana R. and Liu C., ''Thermoelectric power in low-density interstitial-free ıron-aluminum alloys'', ***Philosophical Magazine Letters,*** Vol. 93, No. 9: 502–511, (2013)

**[48]** Sang S., Wang J., Xu B., Lei X., Jiang H., Zhang Q., and Ren Z., ''Thermoelectric properties of n-type $Bi_2Te_{2.7}Se_{0.3}$ with addition of nano ZnO:Al Particles'', ***Materials Research Express*** 1:035901, 1-8, (2014)

**[49]** Elsheikh M.H., Shnawah D.A., Sabri M.F.M., Said S.B.M., Hassan M.H., Bashir M.B.A. and Mohamad M., ''A review on thermoelectric renewable energy: principle parameters that affect their performance'', ***Renewable and Sustainable Energy Reviews,*** 30 :337–355, (2014)

**[50]** Cheng H., Xu X.J., Hng H. and Ma J., ''Characterization of Al-doped ZnO thermoelectric materials prepared by RF plasma powder processing and hot press sintering'', ***Ceramics International***, 35 :3067-3072, (2009)

**[51]** Krishna S.C., Supriya A.K., Pant B., Sharma S.C., and George K.M., '' Thermal conductivity of Cu-Cr-Zr-Ti alloy in the temperature range of 300–873K'',***International Scholarly Research Network ISRN Metallurgy,*** Volume 2012: 580659, 4 pages, (2012)

**[52]** He Z., Platzek D., Stieve C., Chen H., Karpinski G., and Müller E., ''Thermoelectric properties of hot-pressed Al- and Co-doped ıron disilicide materials'', ***Journal of Alloys and Compounds,*** 438: 303–309, (2007)

**[53]** Broudouy B. and Four A. ''Low temperature thermal conductivity of aluminum alloy 5056'', ***Cryogenics***, 60:1-4, (2014)

**[54]** Kuo Y.K., Lue C.S., Hsu G., Huang J.Y. and Hsieh H.L., '' Investigation of Al substitution on the thermoelectric properties of $SrSi_2$'', ***Materials Chemistry and Physics***,137: 604-607, (2012)

**[55]** Pan L., Qin X.Y., Xin H.X., Song C.J., Wang Q., Sun J.H., and Sun R.R., '' Effect of silicon condition on thermoelectric properties of bulk $Zn_4Sb_3$ at low temperatures'', ***Solid State Science,*** 12: 1511-1515, (2010)